



Numerical Analysis of the Continuous Composite Slab Strengthened by CFRP Laminate in the Hogging Moment Region

Khalid W. Dahham¹, Shahrizan Baharom^{1*}, Mohamed S. Majdub¹

¹ Smart and Sustainable Township Research Centre, Faculty of Engineering and Built Environment, Universiti Kebangsaan Malaysia, UKM 43600, Bangi, Selangor DE, Malaysia

*Corresponding Author E-mail: shahrizan@ukm.edu.my

Abstract

In this study, 3-D finite element models were used to investigate the performance of a continuous composite slab (CCS) with profiled steel sheet strengthened by CFRP laminates in a negative moment region. FE models were validated using available experimental data before being used for parametric studies. The parameters were the number of CFRP, slab thickness and concrete strength. The results obtained from the finite element analysis of the strengthened CCS models agreed well with the experimental tests where the deviation in the ultimate hogging moment is only between -2.0% and $+3.0\%$. It proved that the developed FE model is capable of simulating the CCSs strengthened in the hogging region by CFRP laminate. Results have shown that the strengthening of the CCS specimen in the hogging region with CFRP laminates significantly improved its moment capacity about 23% and 91% using one and three CFRP laminate, respectively. Furthermore, increased in slab thickness and concrete strength resulted in higher load improvement.

Keywords: Continuous composite slab, carbon fibre-reinforced polymer, hogging moment.

1. Introduction

Continuous composite slabs have great interest by many researchers because of their many structural characteristics compared with the equivalent reinforced concrete slab, for example, greatest strength, stiffness, and load capacity. Furthermore, the use of continuous composite slabs (CCS) with profiled steel sheet will reduce the construction time and cost as the shuttering system is not required. The profile steel sheet supports the concrete slab during the casting time, as well as it acts as the external reinforcement later. In CCS, profiled steel sheet will act as reinforcement to resist moment curvature at mid-span, while additional reinforcement needed to be added to resist negative moment at intermediate support [1-3]. Moreover, the moment resistance of CCS at intermediate supports could not be sufficient, especially when the ratio of reinforcement to concrete is small [4] and will lead to concrete cracks, and moment redistribution [1]. In designing of simply supported composite slabs, reinforcements to prevent the cracks were added at tension area with not less than 0.2% of the concrete cross-sectional area above the sheet's ribs [2]. Agbossou et al. [5] conducted a numerical analysis using ANSYS software program to simulate the bending behaviours of slabs strengthened by CFRP strips. The proposed model was used to study the influence of the concrete that was covering the steel upon the bending behaviours of the slabs reinforced by FRP.

Nowadays, carbon fibre-reinforced polymer (CFRP) laminate is normally used in rehabilitation of concrete structures due to its advantages such as easy to apply, high modulus of elasticity, resistance to corrosion, and high in tensile strength. Many studies were conducted to study the capability of using CFRP laminates/ plates as strengthening materials in concrete beams and slabs [6- 10]. To the author's knowledge, not many studies focused on applying CFRP in composite structures available [11] especially on the composite floor with profiled steel sheeting.

In this study, CFRP was used in the continuous composite slab (CCS) with profiled steel sheet in the hogging moment region purposely to increase the tensile capacity of the system without placing additional reinforcement bar. This is very useful especially for upgrading the capacity of the slab, especially in the rehabilitation process of the buildings. Furthermore, the finding also can be used for a new construction where the depth of the slab needed to be reduced with additional tensile capacity. Although the composite floor utilizing profiled steel sheeting is widely been investigated, none of the design recommendations is given in using CFRP in the composite floor. FE models were developed and verified against experimental results [12]. The parameters investigated were the number of CFRP, slab thickness and concrete strength.

2. Review of the experimental program

The experimental test results as in [12] were used to validate the developed finite element model. Two specimens of continuous composite concrete-deck slab consisting of two spans, CCS and CCS-1.7L, were chosen for validation purpose. CCS specimen is the continuous com-



posite slab without CFRP acting as control slab. CCS-1.7L represents as the continuous composite slab strengthened with 1.7 m length of CFRP. The CFRP laminate was applied on the top of concrete at the intermediate support (hogging moment region), as shown in Figure 1. Table 1 describes the details of the specimens tested.

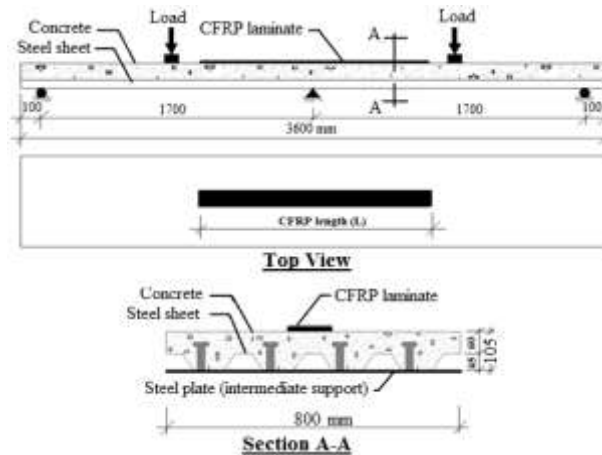


Fig 1: The specimens of the strengthened continuous composite slab (all dimensions in millimetres). [12]

Table 1: Details of the specimens tested.

Specimen	CFRP length, L (m)	Concrete compressive strength, f_{cu} (MPa)	Width (mm)	Thickness (mm)	Effective slab length (mm)
CCS	–	30.2	800	105	3600
CCS-1.7L	1.7	30.1	800	105	3600

3. Numerical Analysis.

3.1 Finite Element Modelling

Nonlinear FE models were developed using ANSYS software [13] to simulate the CCS strengthened with CFRP laminate in the hogging region. The configuration of the CCS FE model was similar to the experimental test. Figure 1 shows the typical FE model, including the loading and boundary conditions assigned in this study. The load option was adopted for all FE models to implement the applied point loads and was gradually increased until the models achieved their ultimate load capacities (i.e., the CFRP of the strengthened models was delaminated). Four different materials were adopted for each FE strengthened model (concrete, profile steel sheet, epoxy, and CFRP laminate). To implement the concrete material, a 3-D solid element (SOLID65) was selected since it has three degrees of freedom at each node and because this element is capable of cracking under tension stress and crushing under high compression stress. A shell element with four nodes named SHELL181 was used to model the profile steel sheets; this element is well-suited for linear, large rotation, and/or large strain nonlinear applications. The element type SOLID185 was used to implement the CFRP laminate. This element is defined by eight nodes having three degrees of freedom at each node translation in the nodal x, y, and z directions and also has plasticity, hyperelasticity, stress stiffening, creep, large deflection, and large strain capabilities. In general, this element (SOLID185) has a mixed formulation capability for simulating deformations of nearly incompressible elastoplastic materials and fully incompressible hyperelastic materials. The adhesive material was considered as an independent layer [5,8,14] and the element type SOLID65 was adopted. Full bond interaction has been assumed between the steel sheets and concrete surfaces because limited end-slip of concrete was recorded due to the application of shear studs to the tested specimens. Also, full interactions between the concrete and epoxy elements and between the epoxy and CFRP elements are considered, where the epoxy elements (SOLID65) effectively implemented the debonding failure in this study.

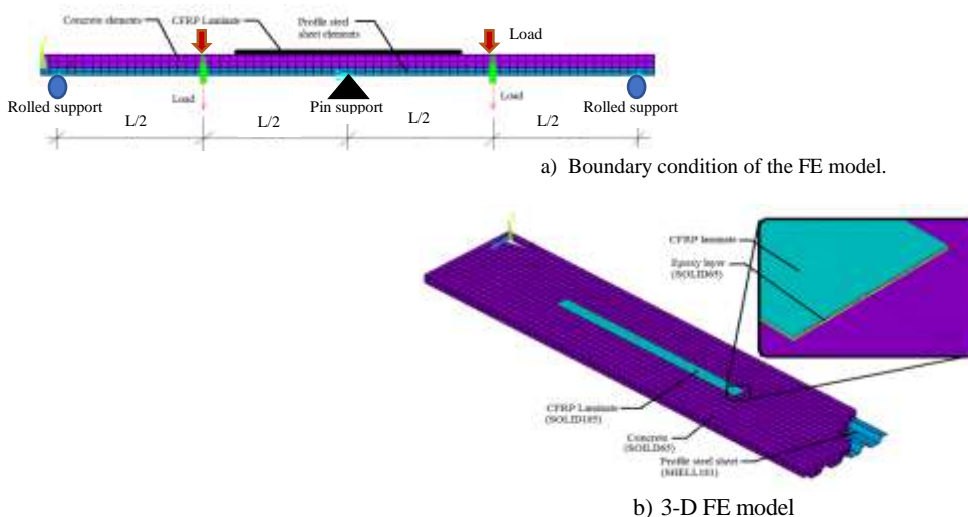


Fig 1: FE modelling of the proposed composite slab system.

Concrete is defined as a brittle material that has two failure mechanisms: crushing behaviour under compression stress and cracking behaviour under tensile stress. A multi-linear uniaxial stress-strain relationship is adopted for the compression and tension strengths of concrete as shown in Figure 2 (a). The relationship depicted by the stress-strain concrete curve is assumed to be based on the numerical equations (1) and (2), which were suggested by [15]. A maximum strain ϵ_u of concrete of 0.0035 and a Poisson's ratio equal to 0.2 were used.

$$f = \frac{E_c \epsilon}{1 + \left(\frac{\epsilon}{\epsilon_0}\right)^2} \quad (1)$$

$$\epsilon_0 = \frac{2f_{cu}}{E_c} \quad (2)$$

$$E_c = 4700\sqrt{f_{cu}} \quad (3)$$

Where E_c is Modulus Young of concrete and ϵ is an ultimate strain in tension.

After the maximum stress (f_{cu}) point, the softening branch stress-strain curve approaches a perfectly plastic behaviour to overcome convergence problems. The von Mises yield criterion was used to model the plasticity. The value of tensile strength of concrete is assumed to be linear before cracking and equal to the splitting tensile strength (f_{ct}) proposed by [16].

$$f_{ct} = 0.56\sqrt{f_{cu}} \quad (4)$$

The behaviour of the profile steel sheet in both tension and compression is assumed to be elastic-perfectly plastic as shown in Figure 2(b). The pattern is chosen to agree with actual stress-strain curves obtained from tension tests of steel sheet coupons. The von Mises yield criterion is used with the associative flow rule and isotropic hardening rule. Poisson's ratio for cold-formed steel is assumed to be equal to 0.3.

The unidirectional CFRP laminate was modelled as a linear elastic orthotropic material (Obaidat et al., 2010). The stress-strain relationship for unidirectional fibre laminates is linearly elastic up to the rupture limit (see Figure 2(c)). The adhesive behaviour is considered as elastic-perfectly plastic material under tensile stress. In general, the same material properties as for the CCS specimens tested experimentally in this study were used to develop the FE models.

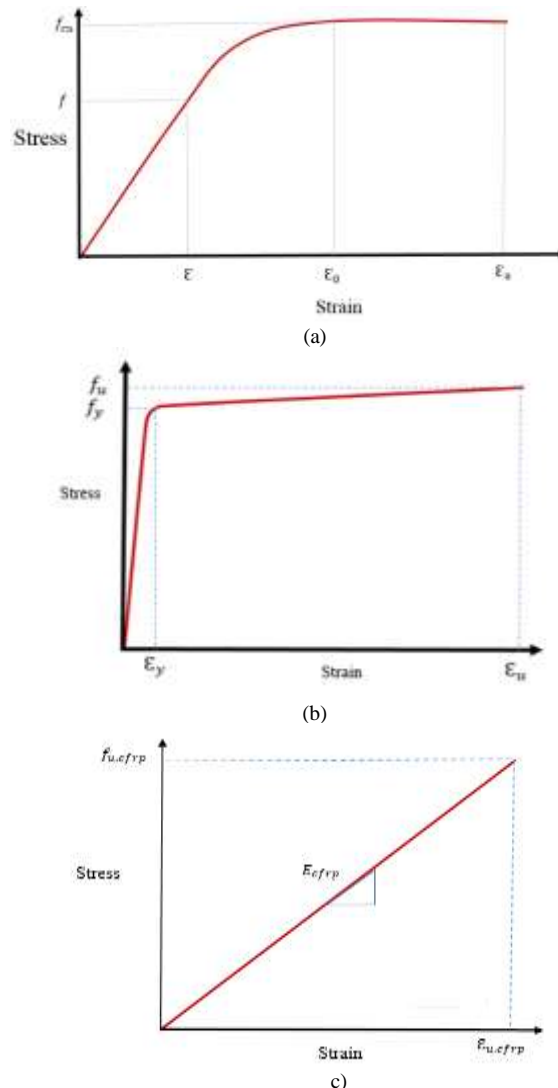


Fig 2: Stress-strain relationships of materials; a) Concrete, b) Profiled steel sheet, c) CFRP Laminate

3.2 Verifying the FE models

The validity of the developed FE models confirmed the experimental results for the CCS specimens. Figure 3 presents the moment versus mid-span deflection curves obtained from the FE analysis and the experimental tests of the specimens CCS and CCS-1.7L as examples. Generally, the FE models achieved close trends in moment-deflection curve corresponding to experimental one within acceptable deviations in ultimate moment capacity, which were about +3.0% and -2.0% for the models of CCS and CCS-1.7L, respectively. Figure 4 provides an FE illustration of the failure behaviour of the strengthened CCS models, which matched the actual behaviours of the corresponding experimental specimens fairly well [12]. Therefore, from the above verification study, it was concluded that the developed FE model is capable of simulating the CCSs strengthened in the hogging region by CFRP laminate.

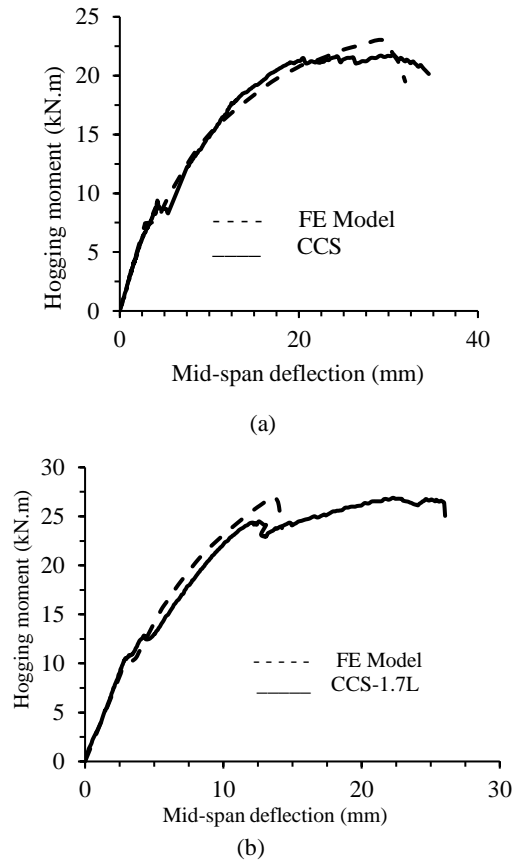


Fig 3: Moment-deflection verification of slab specimens with FE Model; (a) CCS and (b) CCS-1.7L.

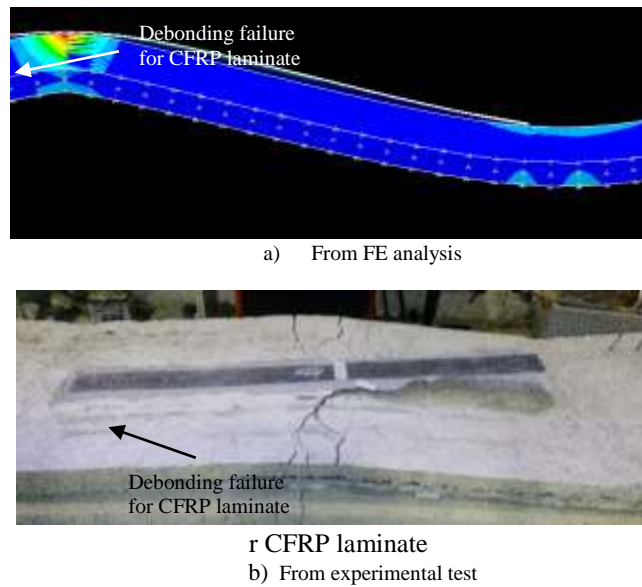


Fig 4: CFRP failure mode for the FE model and experimental specimen CCS-1.7L.

3.3. Parametric studies

After the adequacy of the developed FE models had been confirmed, further parametric studies were conducted numerically to investigate the strengthening behaviour of CCS by using the CFRP laminates, including the effects of slab thickness, concrete strength, and the

number of CFRP laminates used per slab width. Unless otherwise specified, all material properties and boundary conditions for the suggested FE models remained the same as for the verified models.

3.4. Effect of slab thickness.

This section investigates the effect of slab thickness on the performance of CFRP laminate used for strengthening the CCS. Generally, the thickness of the composite slab was limited to not less than 80 mm [2]. Ten FE models with varying slab thicknesses were used (85, 95, 105, 115, and 125 mm), as shown in Figure 5. Two FE models were considered for each thickness: one for the control model and another for the strengthened model with a CFRP laminate length of 1.7 m. An additional number was added to the FE model ID to represent the change in the slab thickness: “85T”, “95T”, “105T”, “115T”, or “125T”, as shown in Table 1.

The results obtained from the FE analysis showed that the influence of CFRP laminates increases with increasing slab thickness up to a certain limit, as shown in Figure 6 and Table 1. For example, the CCS model with a slab thickness of 85 mm (CCS-85T) achieved an LIR equal to 1.176 when strengthened from the hogging region using 1.7 m of CFRP laminate (CCS-1.7L-85T). This LIR value increased to 1.210 when the same CFRP strengthening scenario was used for the same CCS but with a thickness of 95 mm (from models CCS-1.7L-95T and CCS-95T), and then the LIR increased to 1.232 and 1.357 when the concrete slab thickness increased further to 105 and 115 mm, respectively. However, when the slab thickness increased to more than 115 mm, only a small load improvement was achieved, with the LIR value reaching about 1.354 for the models with a slab thickness of 125 mm. In general, increasing the slab thickness of the control CCS models led to an increase in their hogging moment capacity, which is logical behaviour since the thicker concrete cross-section usually has a larger area able to resist the compression stress (area under the neutral axis (N.A); see Figure 7(a). Moreover, when a CFRP plate is applied in the hogging region, it will effectively carry the tension stress at the top surface of the concrete, and thus the N.A will move upward slightly, allowing a larger area of the concrete cross-section to carry the compression stress, as shown in Figure 7(b).

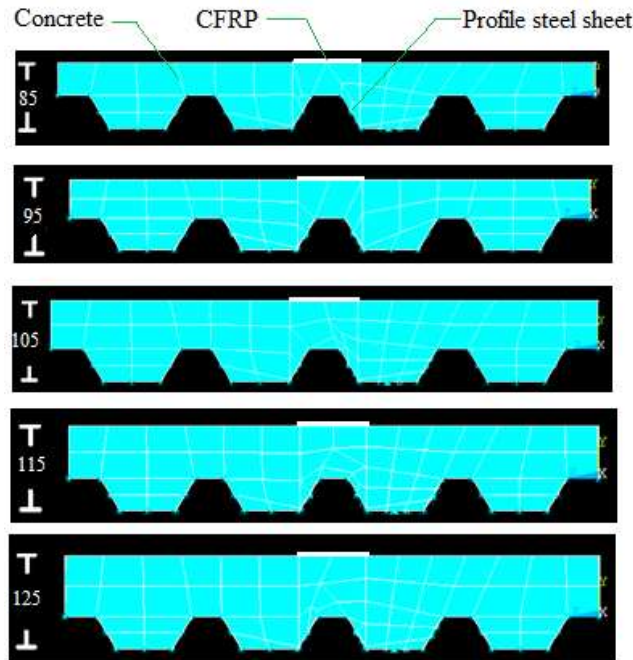


Fig 5: Cross-section of CCS FE models with different slab thicknesses.

Table 1: Load improvement ratio of CCS models with varying slab thickness

Model	Slab Thickness, t (mm)	Ult. Moment Of Control Model, M_{uc} (kNm)	Ult. Moment of Strengthened Model, M_{us} (kNm)	LIR
CCS-85T	85	15.3	–	–
CCS-1.7L-85T	85	–	18.0	1.18
CCS-95T	95	18.5	–	–
CCS-1.7L-95T	95	–	22.4	1.21
CCS-105T	105	22.0	–	–
CCS-1.7L-105T	105	–	27.1	1.23
CCS-115T	115	23.1	–	–
CCS-1.7L-115T	115	–	31.4	1.36
CCS-125T	125	26.3	–	–
CCS-1.7L-125T	125	–	35.6	1.35

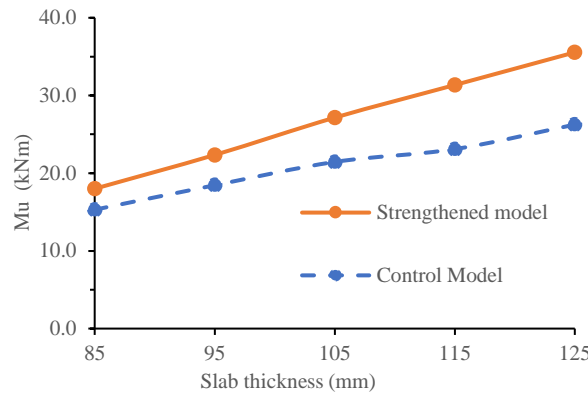


Fig 6: Ultimate moment capacity (M_u) of CCS with different overall slab thicknesses.

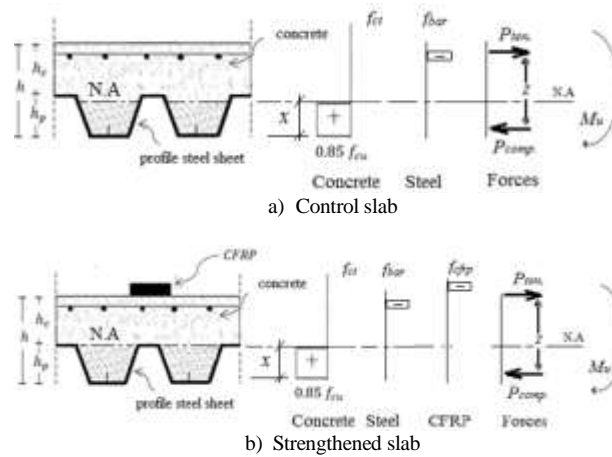


Fig 7: Stress distribution at the intermediate support (moment in the hogging region)

3.5 Effect of concrete strength

This section investigates and discusses the effect of concrete strength on the strengthening behaviour of CCS models when using CFRP laminates. Ten FE models with various concrete strength of CCS were used (20, 25, 30, 35, and 40 MPa). Also, two FE models were analysed for each of the suggested concrete strength values (control and strengthened models). An additional number was added to the FE model ID to represent the change in the concrete strength: 20C, 25C, 30C, 35C, or 40C, as shown in Table 2.

The influence of the CFRP laminates also increased with increasing concrete strength up to a certain limit because of the enhancement, as shown in Figure 8 and Table 2. The CCS model with a concrete strength of 20 MPa (CCS-20C) achieved an LIR equal to 1.144 when strengthened with 1.7 m of CFRP laminate (CCS-1.7L-20C). Then, this LIR value increased to 1.219 and 1.232 when the same strengthening scenario was used for the same CCS but with higher concrete strengths of 25 and 30 MPa, respectively, in models CCS-1.7L-25C and CCS-1.7L-30C. However, when the concrete strength increased to more than 30 MPa, the increment in the LIR value was very limited: the CCS models with concrete strengths of 35 and 40 MPa achieved LIR values equal to 1.307 and 1.284, respectively. This is because the slab with higher concrete strength usually achieved a higher compression force (P_{comp}) than the slab with lower strength when their N.As were at the same level (see Figure 7(b)), which led to a higher M_u value. Using CFRP laminate to strengthen CCS with a high-strength concrete will be more effective than in the case of low-strength concrete, as the performance of CFRP laminate was effective and enhanced the whole behaviour of the slab [18].

Table 2: Load improvement ratio of CCS models with varying concrete strength.

Model	Concrete Strength (f_{cu}) (MPa)	Ult. Moment of Control Model, M_{uc} (kNm)	Ult. Moment of Strengthened Model, M_{us} (kNm)	LIR
CCS-20C	20	18.8	—	—
CCS-1.7L-20C	20	—	21.5	1.14
CCS-25C	25	20.6	—	—
CCS-1.7L-25C	25	—	25.1	1.22
CCS-30C	30	22.0	—	—
CCS-1.7L-30C	30	—	27.1	1.23
CCS-35C	35	24.1	—	—
CCS-1.7L-35C	35	—	31.5	1.31
CCS-40C	40	26.2	—	—
CCS-1.7L-40C	40	—	33.6	1.29

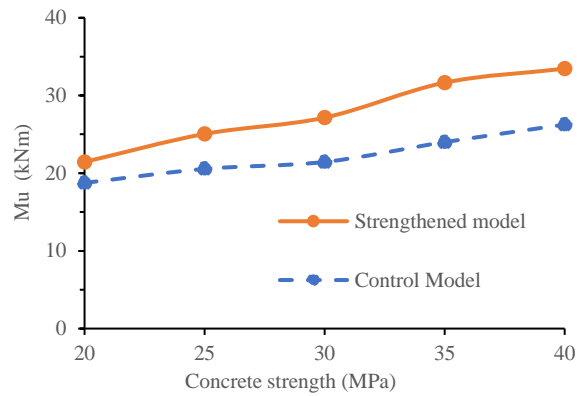


Fig 8: The hogging M_u of the strengthened CCS model with varying concrete strength.

3.6 Effect of number of CFRP

The effect of using more than one CFRP laminate to strengthen the CCS models was investigated as well. The same CCS model as was used for the verification study has been used in this section, and additional CCS models strengthened with different numbers of CFRP laminates per width (one, two, or three CFRP laminates) were developed. These CFRP laminates were placed in parallel along the slab length and distributed equally in the width direction, as shown in Figure 9. In general, the results clearly confirmed that increasing the total number of CFRP laminates per CCSs width significantly improved their hogging moment capacity (M_u). This is because the total effective cross-sectional area of CFRP was increased, which led to an increase in the tension force (P_{ten}) in Figure 7(b)). The M_{uc} value of the control CCS model was about 21.5 kNm, and this value increased to 27.2 kNm when one CFRP laminate was used, achieving an LIR equal to 1.232. This LIR value increased further to 1.811 and 1.963, respectively, when two and three CFRP laminates were used, as presented in Table 3.

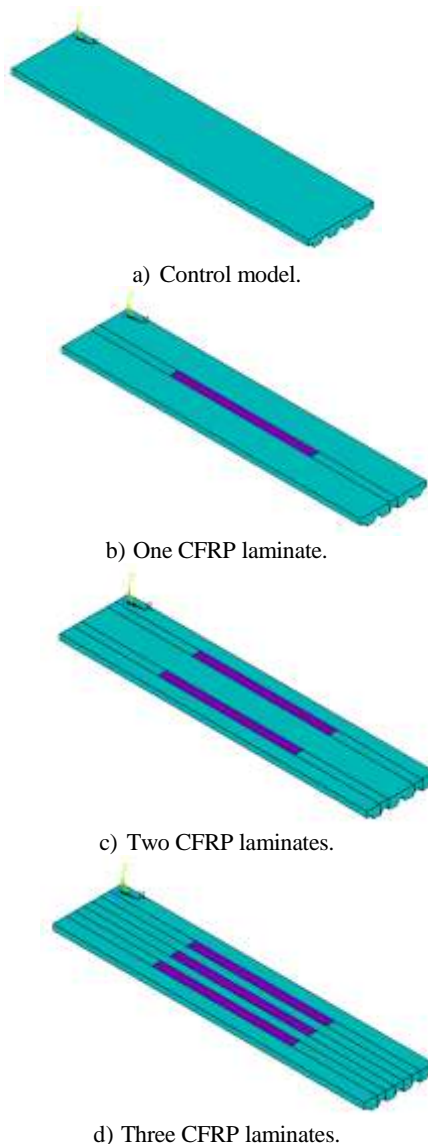


Fig 9: CCS models strengthened with different numbers of CFRP laminates.

Table 3: Load improvement ratio of CCS models with different numbers of CFRP laminates.

Model	Number of laminates	Ult. Moment of Control Model, M_{uc} (kNm)	Ult. Moment of Strengthened Model, M_{us} (kNm)	LIR
CCS	–	22.0	–	–
CCS-1.7L-1F	1	–	27.1	1.23
CCS-1.7L-2F	2	–	38.8	1.81
CCS-1.7L-3F	3	–	42.0	1.96

4. Conclusion

Numerical analyses have been carried out in this research to investigate the performance of continuous composite slab (CCS) when strengthened in the hogging region by CFRP laminates/plates. Several parameters were investigated, including slab thicknesses, concrete strengths and numbers of CFRP laminates per effective slab width. The conclusions obtained from the analyses can be summarized as follows:

- 1- The results and behaviours obtained from the finite element analysis of the strengthened CCS models agreed well with those found by the experimental tests, and the results were within the acceptable deviations (–2.0 to +3.0%).
- 2- In general, strengthening the CCS specimen in the hogging region (the top surface of the concrete at the internal support) with CFRP laminates improved its moment capacity.
- 3- Logically, increasing the slab thickness of the CCS models led to an increase in their hogging moment capacity, since the thicker concrete cross-section usually has a larger area able to resist the compression stress. Moreover, applying for the CFRP plate in the hogging moment region will effectively carry the tension stress at the top surface of the concrete, and thus the neutral axis of the slab cross-section will move upward slightly, allowing a greater concrete area to carry the compression stress.
- 4- Increasing the number of CFRP laminates per slab width in the hogging region significantly increased the moment capacity of the strengthened CCS, because the total effective cross-sectional area of CFRP was increased, which led to an increase in its tension force.

Acknowledgements

The authors would like to express their gratitude to Universiti Kebangsaan Malaysia (UKM) and Ministry of Higher Education (MOHE) and for providing funding to this project with the grant nos. GUP-2018-30 and FRGS/1/2017/TK01/UKM/02/3.

References

- [1] Abas FM, Gilbert RI, Foster SJ & Bradford MA (2013), Strength and serviceability of continuous composite slabs with deep trapezoidal steel decking and steel fibre reinforced concrete. *Engineering Structures* 49, 866–875.
- [2] EC4 (2004), 1-1. Eurocode 4: design of composite steel and concrete structures—Part 1.1: General rules and rules for buildings. European Committee for Standardization.
- [3] Gholamhoseini A, Gilbert I & Bradford MA. Ultimate strength of continuous composite concrete slab. Proceedings of the International conference on composite construction in steel and Concrete, No. 7, (2013).
- [4] Ackermann FP & Schnell J. Steel fibre reinforced continuous composite slabs. Proceedings of the International Conference on Composite Construction in Steel and Concrete, No. 6. (2008), pp. 125–137. [http://doi.org/10.1061/41142\(396\)11](http://doi.org/10.1061/41142(396)11).
- [5] Agbossou A, Michel L, Lagache M & Hamelin P (2008), Strengthening slabs using externally-bonded strip composites: analysis of concrete covers on the strengthening. *Composites Part B: Engineering*, 39(7), 1125–1135. <http://doi.org/10.1016/j.compositesb.2008.04.002>.
- [6] Ashour A, El-Refaie S & Garrity S (2004), Flexural strengthening of RC continuous beams using CFRP laminates. *Cement and Concrete Composites*, 26(7), 765–775. <http://doi.org/10.1016/j.cemconcomp.2003.07.002>.
- [7] Kim JJ, Noh H-C, Reda TMM & Mosallam A (2013), Design limits for RC slabs strengthened with hybrid FRP–HPC retrofit system. *Composites Part B: Engineering*, 51, 19–27.
- [8] Limam O., Foret G., & Ehrlacher A (2003), RC two-way slabs strengthened with CFRP strips: Experimental study and a limit analysis approach. *Composite Structures*, 60(4), 467–471.
- [9] Rahimi H & Hutchinson A (2001), Concrete beams strengthened with externally bonded FRP plates. *Journal of Composites for Construction*, February, 44–56.
- [10] Triantafillou TC & Plevis N (1992), Strengthening of RC beams with epoxy-bonded fibre-composite materials. *Materials and Structures*, 25(4), 201–211.
- [11] Al-Zand AW, Badaruzzaman WHW, Mutalib AA & Hilo SJ (2016), The enhanced performance of CFST beams using different strengthening schemes involving unidirectional CFRP sheets: An experimental study. *Engineering Structures*, 128, 184–198.
- [12] Dahham KW, Baharom S, Badaruzzaman WHW, Muhammad N & Al-Zand A (2018), Static structural performance of continuous composite slab strengthened by CFRP laminate in the hogging moment region, *Journal of Engineering Science and Technology (JESTEC)*, 13(6), 1489–1499.
- [13] ANSYS, C (1998), Ansys Inc. Canonsburg, PA, USA.
- [14] Teng X & Zhang YX (2014), Nonlinear finite element analyses of FRP-strengthened reinforced concrete slabs using a new layered composite plate element. *Composite Structures*, 114, 20–29.
- [15] Desayi P & Krishnan S (1964), Equation for the Stress-strain Curve of Concrete. *Journal of the American Concrete Institute*, 61(3), 345–350.
- [16] ACI code. (1963), American Concrete Institute. Farmington Hills, MI (Vol. 48333).
- [17] Obaidat Y T, Heyden S & Dahlblom O (2010), The effect of CFRP and CFRP /concrete interface models when modelling retrofitted RC beams with FEM. *Composite Structures*, 92(6), 1391–1398.
- [18] Ei-Shihy AM, Fawzy HM, Mustafa SA & El-Zohairy AA (2010), Experimental and numerical analysis of composite beams strengthened by CFRP laminates in hogging moment region. *Steel and Composite Structures*, 10(3), 281–295.